International Journal on
"Technical and Physical Problems of Engineering"
(IJTPE)
Published by International Organization of IOTPE

ISSN 2077-3528
IJTPE Journal
www.iotpe.com
ijtpe@iotpe.com

December 2016 | Issue 29 | Volume 8 | Number 4 | Pages 44-51

THERMODYNAMIC ANALYSIS OF A PROPOSED TRI-GENERATION SYSTEM

A.R. Salimi

Institute of Physics, Azerbaijan National Academy of Sciences, Baku, Azerbaijan, rikani1966@outlook.com

Abstract- The purpose of this study is to develop a method to provide an application to a better thermodynamic analysis of tri-generation system. The system is made of four major components including gasifier, gas turbine, Kalina cycle and refrigeration absorption cycle. Using a creative combination of physics, chemistry and mathematics and considering their relationships, it is attempted to introduce an application to analyze tri-generation system. The result showed that the Kalina cycle was useful to increase the performance of gas turbine and Rankin. To reduce CO_2 emissions and improve exergy efficiency, the application of a combined gas turbine and Kalina cycle found to be effective. Exhausted gas of the combined gas turbine and Kalina cycle yields a large amount of heat which can be recycled to generate power so that the Kalina cycle was used for this purpose. Energy and exergy analysis indicated that in the presence of combined Kalina cycle, the net output was 1.27%, and the efficiency of the first and second law increased by about 54% and 51%, respectively. In addition, it was found that the emission of CO_2 into the atmosphere reduced by 1.24%. Moreover, improved exergy efficiency and CO_2 emissions drop were examined mathematically.

Keywords: Thermodynamic, Tri-Generation System, Kalina Cycle, CO_2 Emissions.

I. INTRODUCTION

The amount of available energy resources and global warming are two important concerns toward the stability of the global energy generation in the future. Therefore, the design of small-scale refrigeration systems with primary drivers such as micro-turbines, spark ignition engines and other types of internal combustion engines has given lots of attention. Using the waste heat from primary driving systems, the systems can be widely used to produce cooling in residential and commercial areas. Power plays an important role in the development of human societies and scientists believe that the way of using the energy resources greatly contributes in nations' development [12].

In 1980, Dr. Alexander Kalina introduced a cycle with a two-component working fluid (water and ammonia) which was named "the Kalina cycle" in his honor. The Kalina cycle was developed as a combined cycle to be replaced by a simple Rankine cycle with a low thermal source temperature. The most important application of the Kalina cycle is the use of low temperature heat sources such as geothermal, biomass, and so on in power and refrigeration cogeneration cycles, and heat recovery from the exhaust gases of internal combustion engines and gas turbines [12].

The main objective of this study is to use energy of biomass for power generation, heating and cooling and assess carbon dioxide emissions to the environment. Also it is aimed to reduce fossil fuel consumption, particularly due to their damaging effect on the environment.

II. HEATING AND COOLING POWER GENERATION SYSTEM

Figure 1 illustrates a combined system based on biomass combustion and gasification. Biomass and air flow into the gasifier, which is assumed to be insulator, at atmospheric temperature and pressure. Gasification reactor is pseudo-homogeneous performing under atmospheric pressure. The produced biogas leaves the gasifier at T_g gasification temperature and flows into the combustion chamber and the point 3 exhaust gas passes through the gas turbine. In the main heat exchanger, exhaust gas of the gas turbine transfer a small part of their thermal energy to the Kalina cycle fluid before flowing into the high pressure generator. The heated fluid enters the Kalina cycle turbine and produces useful work output and the output fluid releases its heat over two high temperature heat exchangers.

Hot gases of combustion pass through high pressure generator after flowing through the main heat exchanger and pass their heat to absorption refrigeration cycle. This cycle consists of two pressure levels. The dilute solution (flow with high concentrations of refrigerant) leaves the absorbent and passes through the pump and goes into the generator after flowing through the low temperature heat exchange. The solution absorbs heat from the generator and water vapor is separated from dilute solution and concentrated fluent passes into the absorber by means of the expansion valve. As Figure 1 shows the overall system consists of three major sections:

- Gasifier and combustion gas in the ignition chamber and gas turbine
- Kalina Cycle
- Lithium-bromide refrigeration cycle

Formulation and assumptions in three major sections of the thermodynamic system are presented and discussed below.

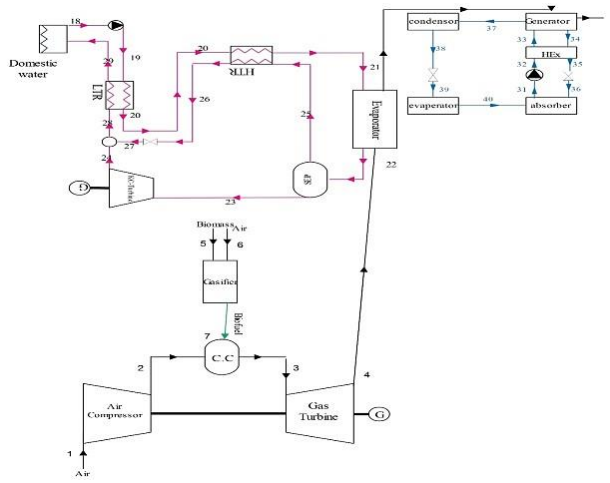

Figure 1. A combined system based on biomass combustion and gasification

A. Gasifier and Gas Turbine

In this paper, the following assumptions have been considered:

- Air passes through compressor (100 kPa pressure and 298 K) and preheater under atmospheric condition.
- Adiabatic gasification process and generated gas in chemical equilibrium.
- Both biomasses are considered with 20% moisture
- The isentropic performance of gas turbine and compressor are assumed 89% and 87%, respectively
- Ignition in the combustion chamber is stoichiometric
- The pressure drop in the combustion chamber is 3% of the inlet pressure.

In order to thermodynamically analyze the different components, each component is considered as a control volume working in a steady state which the laws of conservation of mass and first and second thermodynamic are exerted on. Regardless the potential and kinetic energies, it can be expressed as:

$$\sum \dot{m}_{in} = \sum \dot{m}_{out} \tag{1}$$

$$\dot{Q} + \sum \dot{m}_{in} h_{in} = \dot{W} + \sum \dot{m}_{out} h_{out} \tag{2}$$

To examine the quality of system performance based on the second law of thermodynamics, the exergy of all process needs to be determined. Regardless the kinetic and potential effects, it is defined as:

$$\dot{E} = \dot{E}_{ph} + \dot{E}_{ch} \tag{3}$$

where $\dot{E}_{ph}$ and $\dot{E}_{ch}$ signify physical and chemical exergy of the process, respectively. Physical exergy can be calculated as the following:

$$e_{ph,i} = h_i - h_o - T_0 (S_i - S_o) \tag{4}$$

The rate of exergy destruction was calculated using the standard Gouy-Stodola relation. Since the cycle contains chemical reactions in the gasification and combustion chamber, the chemical exergy of each process should also be calculated. Chemical exergy was calculated relative to completed dead state where the composition stays at the reference pressure and temperature. While physical exergy limit was calculated with respect to the restricted dead state [1, 2].

Chemical exergy for biomass was calculated as follows:

$$e^{ch}_{biomass} = \beta LHV_{biomass} \tag{5}$$

where β factor indicates the ratio of chemical exergy of biomass to its low calorific value as follows [3]:

$$\beta = \frac{1.044 + 0.16\frac{Z_H}{Z_C} - 0.34493\frac{Z_O}{Z_C}\left(1 + 0.0531\frac{Z_H}{Z_C}\right)}{1 - 0.4142\frac{Z_O}{Z_C}} \tag{6}$$

where Z_H, Z_C and Z_O signify the weight ratio of hydrogen, carbon and oxygen. Also specific chemical exergy for the mixture of ideal gases (kJ/kmol) was calculated as [1, 4]:

$$e^{ch}_i = \sum_i x_i e^{ch}_{0,i} + \bar{R}T_0 \sum_i x_i \ln x_i \tag{7}$$

where x_i shows the molar ratio of the mixture component and $e^{ch}_{0,i}$ indicates their standard chemical exergy. With the use of the earlier mentioned assumptions, energy balance relationships and exergy of the cycle components, these relationships are presented in Table 1 in Appendix. Moreover, exergy destruction terms for system components are given in Table 2.

B. Thermodynamic Analysis of Gasification

In the gasifier the equilibrium constants will be used which is given as follow.

Entropy balance is generally defined as $dS = \frac{\delta Q}{T} + \delta\sigma$, where by the removal of $\delta\sigma$, and considering the first thermodynamic law and the produced entropy always more than or equal to zero, we will have:

$$TdS - dU - pdV \geq 0 \tag{8}$$

According to Equation (8), with constant U and V, it can be assumed that $dS \geq 0$. Considering the Gibbs function as $G = H - TS = U + PV - TS$ and the previous result, it can be concluded that $dG - Vdp + Sdt \leq 0$, under constant pressure and temperature $dG \leq 0$. It means that Gibbs function is less than or equal to zero under constant pressure or temperature and it reaches to the least amount (0) in the equilibrium condition. Considering an equilibrium reaction as $\nu_A\mu_A + \nu_B\mu_B \leftrightarrow \nu_C\mu_C + \nu_D\mu_D$, K equilibrium constant for ideal gas mixtures can be measured using $\frac{-\Delta G^0}{\bar{R}T}\ln K$, where ΔG^0 indicates the Gibbs function difference for reactants and products at reaction temperature and atmosphere pressure. The equilibrium constant for ideal gases is as follows:

$$K = \frac{n_C^{vc} n_D^{vD}}{n_A^{vA} n_B^{vB}} \left(\frac{P / P_{ref}}{n_{tot}} \right)^{vc+vD-vA-vB} \quad (9)$$

$$\frac{d\psi_{cs}}{dt} = -r_s i_{cs} + u_{cs} \quad (6)$$

The final analysis of the biomass used in this work is given in Table 3. Also Table 4 exhibits the mass balance equations of energy for Kalina cycle. The downward gasifier was used in this study including four regions of drying, thermal decomposition, reduction and combustion. In the equilibrium model it is assumed that all gasification reactions are in thermodynamic equilibrium and pyrolyzed products burn and reach to equilibrium before leaving the gasifier in the reduction area. Reduction reactions in the reduction region include:

$$C + CO_2 \leftrightarrow 2CO \quad (10)$$

$$C + H_2O \leftrightarrow CO + H_2 \quad (11)$$

$$C + 2H_2 \leftrightarrow CH_4 \quad (12)$$

By the combination of Equations (10) and (11), shift reaction will be gained:

$$CO + H_2O \leftrightarrow H_2 + CO_2 \quad (13)$$

The general reaction of gasification is as follows:

$$CH_aO_bN_c + wH_2O + m(O_2 + 3.76N_2) \rightarrow \\ \rightarrow n_1H_2 + n_2CO + n_3CO_2 + n_4H_2O + n_5CH_4 + n_6N_2 \quad (14)$$

where w indicates the number of kilo moles of water per kg of biomass, m the number of kilo moles of oxygen per kilo moles of biomass through the gasification process, n_1 to n_6 show the number of kilo moles of products obtained from biomass gasification. Mass of water to mass of wet biomass can be expressed as:

$$MC = (\text{mass of water / mass of wet biomass}) \times 100 \quad (15)$$

where number of kilo mole of water can be calculated as:

$$w = \frac{M_{biomass} MC}{18 \times (1 - MC)} \quad (16)$$

where $M_{biomass}$ signifies the mass of biomass.

Considering the mass and energy balances in the general equation of gasification and the equilibrium constants to produce methane and gas-water reaction, the n_1 to n_6 values and the T_g gasification temperature (when m is known) and the value of m (when T_g is known) are achieved.

Equilibrium constants for the formation of methane and the shift reaction are expressed as:

$$K_1 = \frac{n_5}{n_1^2} \left(\frac{P / P_{ref}}{n_{tot}} \right)^{-1} \quad (17)$$

$$K_2 = \frac{n_1 n_3}{n_2 n_4} \left(\frac{P / P_{ref}}{n_{tot}} \right)^{0} \quad (18)$$

Equilibrium constants are defined as follows:

$$\frac{-\Delta G_1^0}{\bar{R} T_g} = \ln K_1 \quad (19)$$

$$\frac{-\Delta G_2^0}{\bar{R} T_g} = \ln K_2 \quad (20)$$

where

$$-\Delta G_1^0 = (\bar{h}_{CH_4} - T_g \bar{S}_{CH_4}) - 2(\bar{h}_{H_2} - T_g \bar{S}_{H_2}) \quad (21)$$

$$-\Delta G_2^0 = (\bar{h}_{CO_2} - T_g \bar{S}_{CO_2}) + (\bar{h}_{H_2} - T_g \bar{S}_{H_2}) - \\ -(\bar{h}_{CO} - T_g \bar{S}_{CO}).(\bar{h}_{H_2O} - T_g \bar{S}_{H_2O}) \quad (22)$$

Assuming gas-insulated gasifier of the first law of thermodynamics, the overall gasification reaction can be written as follows:

$$\bar{h}_{f-biomass}^0 + w \times \bar{h}_{f-H_2O}^0 = n_1 \left(\bar{h}_{f-H_2}^0 + \Delta \bar{h}_{H_2} \right) + \\ + n_2 \left(\bar{h}_{f-CO}^0 + \Delta \bar{h}_{CO} \right) + n_3 \left(\bar{h}_{f-CO_2}^0 + \Delta \bar{h}_{CO_2} \right) + \\ + n_4 \left(\bar{h}_{f-H_2O}^0 + \Delta \bar{h}_{H_2O} \right) + n_5 \left(\bar{h}_{f-CH_4}^0 + \Delta \bar{h}_{CH_4} \right) + \\ + n_6 \left(\bar{h}_{f-N_2}^0 + \Delta \bar{h}_{N_2} \right) \quad (23)$$

The right side of the Equation (23) is occurred at gasifier temperature, so that the difference between enthalpies of components from solutions at gasifier temperature and reference temperature will be 298 Kelvin. The enthalpy of biomass formation can be calculated by calorific value (5) or components (7).

C. Thermodynamic Analysis of the Combustion Chamber

Exhaust air from the gas turbine and exhaust biogas flows into the combustion chamber. Assuming the stoichiometric combustion reaction, the equation can be defined as follows:

$$n_1H_2 + n_2CO + n_3CO_2 + n_4H_2O + n_5CH_4 + \\ + n_6N_2 m'(O_2 + 3.76N_2) \rightarrow n_7CO_2 + n_8H_2O + \\ + n_9O_2 + (3.76 n_{air,1}) N_2 \quad (24)$$

where m' shows the number of moles of oxygen input to the combustion zone per kilo mole of wood. Assuming the first law of thermodynamics in combustion chamber area, it can be said:

$$\sum_j N_j \left(\bar{h}_{f_j}^0 + \Delta \bar{h} \right)_{produced\ gas} + \sum_j N_j \left(\bar{h}_{f_j}^0 + \Delta \bar{h} \right)_{Air,1} = \\ = \sum_j N_j \left(\bar{h}_{f_j}^0 + \Delta \bar{h} \right)_{products} \quad (25)$$

where N_j indicates the number of moles of components in the produced gas, air and combustion products.

After passing through the air preheater, the combustion gases flow into the main heat exchanger and convey their heat to the Kalina cycle that is discussed below.

D. Kalina Cycle Assumptions

The assumptions used are as follows:

i. The system works in a steady state.

ii. Frictional pressure drop was trifling and the effects of kinetic and potential energy was ignored.

iii. Domestic water input is used at environment temperature and pressure and the output is at ambient pressure.

E. Kalina Cycle Thermodynamic Analysis

To thermodynamically analyze of the system, each component is considered as the control volume. According to the output and input laws of conservation of and energy and exergy applied to them, they are as follows. The second law of thermodynamics has been applied to the cycle components in order to evaluate the quality performance of cycle, and the equations are listed in Table 5.

F. Lithium-Bromide Absorption Refrigeration Cycle

In order to thermodynamically analyze the refrigeration cycle, each component is considered as a control volume that are exerted on them based on input, output, the laws of conservation of mass, energy and exergy balance relation. The relations are as followings:

Applying the first law of thermodynamic on energy balance equations cycle as Table 6. Also, by applying the second law of thermodynamics cycle on the components of exergy balance equations cycle as Table 7 is obtained.

G. Thermodynamic Analysis of Tri-Generation System

Cycle performance was investigated based on burning rate (one kilogram per second). Efficiency of the first law of the gasification process, known as cold gas efficiency, is shown as below [9].

$$\eta_{cold-gas} = \frac{LHV_{gas}}{LHV_{biomass}} \tag{26}$$

where LHV_{gas} and $LHV_{biomass}$ are low heating value of exhaust gas and biomass, respectively. The LHV_{gas} and $LHV_{biomass}$ are calculated based on one kilogram biomass. Despite the fact that gasifier is assumed to be adiabatic and sensible, exhaust heat is not considered to measure efficiency, the output is usually less than 100%. Cold gas efficiency can have an effect on determining the amount of chemical energy derived from biomass gasification, however neglecting the sensible heat seems to be a weakness point for the cold gas efficiency.

The problem can be solved considering exergy efficiency, which takes the chemical and physical exergy of the produced gas into consideration.

$$\Psi = \frac{\overline{e}_{ch,gas} + \overline{e}_{ph,gas}}{\overline{e}_{ch,biomass}} \tag{27}$$

First Law efficiency of cycle is obtained using specific gas turbine work output and Kalina cycle turbine, compressors, pumps and low calorific value of biomass:

$$\eta_I = \frac{\dot{W}_{net,GT} + \dot{W}_{net,Kalina} - \dot{W}_{pump} + \dot{W}_{heating} + \dot{Q}_{cooling}}{\dot{m}_{biomass} LHV_{biomass}} \tag{28}$$

where, $\dot{W}_{net,GT} = \dot{W}_{net} - \dot{W}_{AC}$.

The waste heat is done through exhaust gas of the cycle within cooling liquid in the refrigeration cycle. Combined triple generation input exrgy ($\dot{E}_{in}$) per kilo mole biomass is given as:

$$\dot{E}_{in} = e^{ch}_{biomass} + we^{ch}_{water} + 4.76(m+m')e^{ch}_{air} \tag{29}$$

A portion of the exergy is converted into useful work, some portion is spent on heating and refrigeration, and the rest is destroyed because of the irreversibility in the components of the cycle or released as the exhaust gas. Exergy efficiency of the CCHP cycle is defined as follows:

$$\varepsilon = \frac{\dot{W}_{net,GT} + \dot{W}_{net,Kalina} + \dot{E}_{heating} + \dot{E}_{cooling}}{\dot{E}_{in}} \tag{30}$$

where $\dot{E}_{cooling}$ is given as:

$$\dot{E}_{cooling} = \dot{Q}_{cooling}\left(\frac{T_0 - T_{evap}}{T_{evap}}\right) \tag{31}$$

III. RESULTS AND DISCUSSION

A. Thermodynamic Analysis of CCHP

Different components of the studied cycle (gasifier, gas turbine, Kalina cycle and absorbent-refrigeration cycle) were validated and the results are provided as below.

The constituent of the produced gas emitted from wood gasification under 20% moisture and 1073 K temperature are provided in Table 8. As compared to the results reported by other authors (Table 8), our findings were parallel with those reported by Zainal [5]. The total amount of hydrogen and carbon monoxide, which plays an important role in calorific value, found to be 42.08% which is in consistent with the values of empirical results (38.3%). Based on the results, the value of hydrogen was more but carbon monoxide was less than that of the empirical results.

The obtained results of the present study compared with the empirical results and the value of wood gasifier at 20% moisture and 1073 K are exhibited in Table 8.

Also the results for gas turbine and gasifier gained through validation were in conformity with those reported by other authors [12].

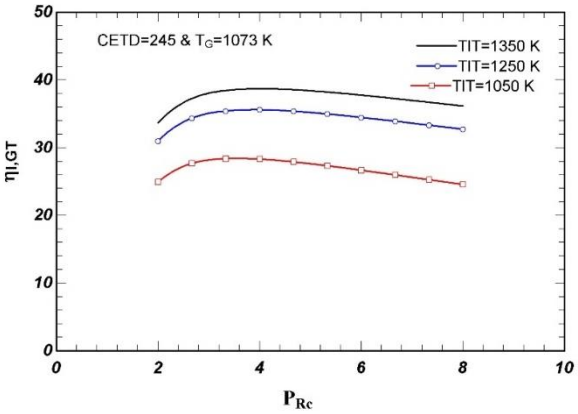

Figure 2. validation of the gas turbine with gasifier

B. Kalina Cycle Modeling Validation

Moreover, the empirical results in the literature were used in order to validate the findings of Kalina cycle modeling (S-CO_2). For this purpose, the results found by Gholamian et al. [13] were used for comparison.

C. Lithium-Bromide Absorption Refrigeration Cycle Modeling Validation

To validate Lithium-bromide absorption refrigeration cycle, the results were compared with those of Ghamari et al. [18] which were proven to be consistent.

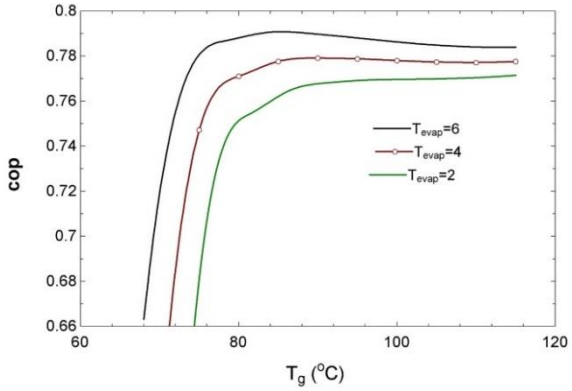

Figure 3. Lithium-bromide absorption refrigeration cycle modeling validation (circles show the results gained by other studies)

D. Results of the Parametric Study

Results of the important decision parameters that show the basic behavior of the system are given. Figure 4 depicts the change in the first and second law efficiency of the power generation system with the ratio of pressure. Based on the figure, it can be seen that the efficiency values are optimized at a specific pressure ratio that equals 32.33% and 26.87% for the first and second law, respectively. The reason is that turbine work increases to a certain pressure ratio; however increased input work of compressor outweighs the turbine output work.

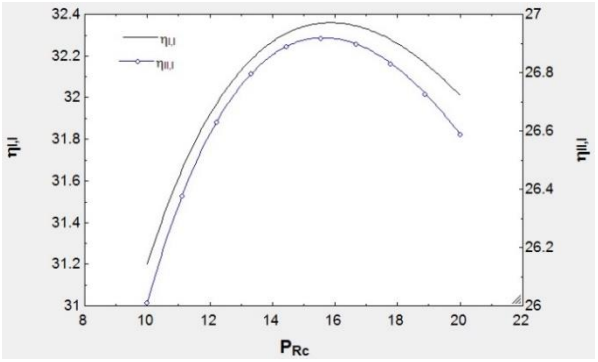

Figure 4. Change in the first and second law efficiency of power generation system with pressure ratio

Figure 5 shows the change in efficiency of the first and second law of power generation system with gas turbine inlet temperature. It shows that the efficiency of both the first and second law efficiency increases with gas turbine inlet temperature. The reason is obvious because the gas turbine inlet temperature is as same as the exhaust system upstream temperature. According to Carnot system efficiency, the more heat source temperature, the higher system efficiency. By increasing the system temperature to 400 ºC, the first law and the second law efficiency increase to 9.9% and 6.9%, respectively.

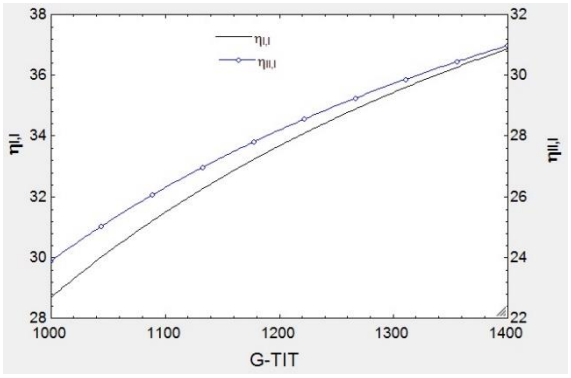

Figure 5. Change in the first and second law efficiency of the power generation system with gas turbine inlet temperature

Figure 6 shows the change in the cold gas efficiency, besides the second law with the gas temperature. The cold gas efficiency showed opposite trend than the second law efficiency. As temperature rises, the cold gas efficiency increased according to Eq. 26, but the second law efficiency showed no rise due to the reduced irreversibility of the temperature difference.

By increasing the gasification temperature by 250 Cº, the second law efficiency increased to 7.0%, but cold gas efficiency fell to 0.12%.

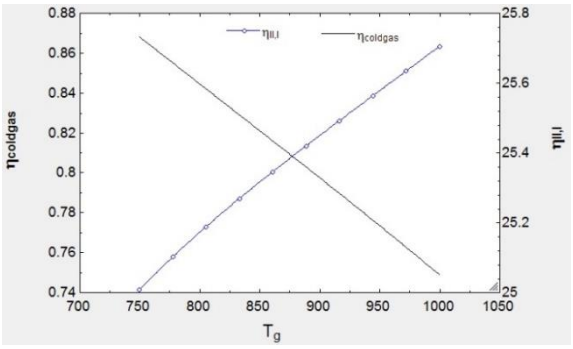

Figure 6. Change in the cold gas efficiency and the second law with gasification temperature

The change in the first and second law efficiency of the Kalina cycle with mixing rate of turbine inlet is given in Figure 7. According to the figure, it is clear that increased rate of mixed input ammonia (to 0.2) to Kalina turbine improves the efficiency. In addition, the first and second law efficiency increased to 17.9% and 29.5%, respectively.

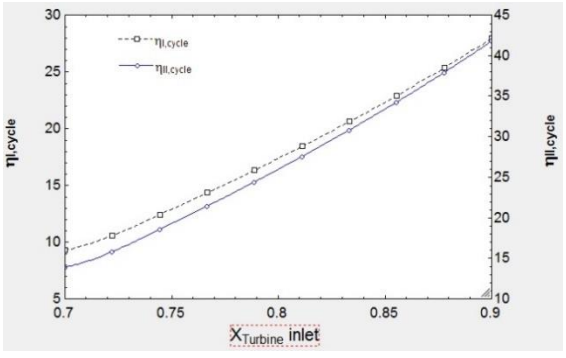

Figure 7. Change in the first and second law efficiency of the Kalina cycle with varied ratio of input to turbine

Figure 8 shows the change in the first and second law efficiency of the Kalina cycle the turbine inlet pressure. The figure shows that the first and second law efficiency is optimized by increasing the pressure at certain points which is identical with that of Rankine cycle power. The optimal values for the first and second law were 21.2 and 31.9, respectively while the optimized turbine inlet pressure was 16.2.

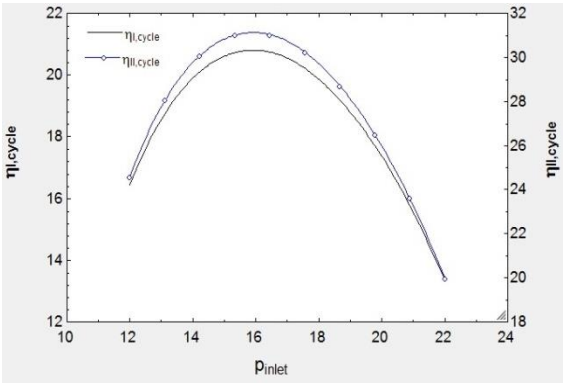

Figure 8. Change in the first and second law efficiency of the Kalina cycle with turbine inlet pressure

The change in the first and second law efficiency of the Kalina cycle with turbine inlet temperature is exhibited (Figure 9). A high temperature source was considered for turbine inlet temperature in the Kalina cycle. Therefore, the efficiency of the cycle increases with the Carnot cycle efficiency. By 20 ºC increment in the turbine inlet temperature for Kalina cycle, the first and second law efficiency increased by 10% and 15.5%, respectively.

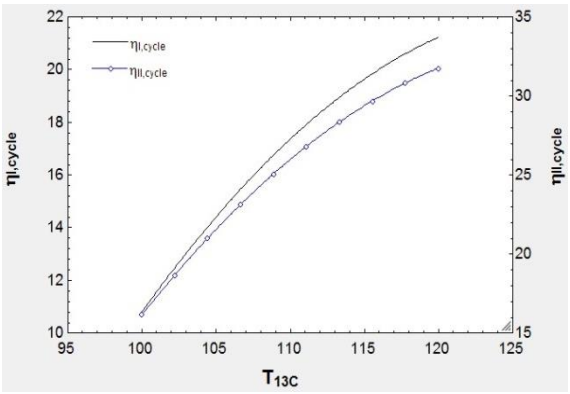

Figure 9. Change in the first and second law efficiency of the Kalina cycle with turbine inlet temperature

Performance of the efficiency coefficient of the refrigeration cycle with the generator temperature has been shown in Figure 10. The trend of system is increasing first and then decreasing. The coefficient of performance changed into 0.77 by increasing the temperature from 80 to 110 ºC.

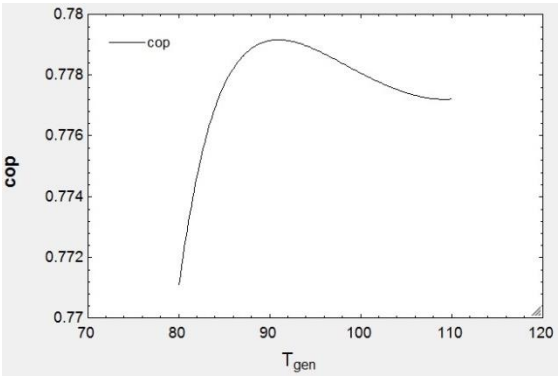

Figure 10. Performance of the efficiency coefficient of the refrigeration cycle with the generator temperature

E. Exergy Analysis Results

Figure 11 shows the rate of exergy destruction of the hybrid system components. The maximum values of the exergy destruction and combustion chamber were 2440 and 5395 kW, respectively. The reason is that they contain all three sources of irreversibility i.e. temperature difference, friction and chemical reactions.

The gas turbine has got the third place, because the high rate of exergy enters the system and consequently it will have high exergy destruction.

Exergy destruction in each component is calculated using the Gouy-Stodola equation. As shown in Figure 11, exergy destruction rates of other components found to be lower, because exergy input into the system is much less than the high level exergy of the inlet.

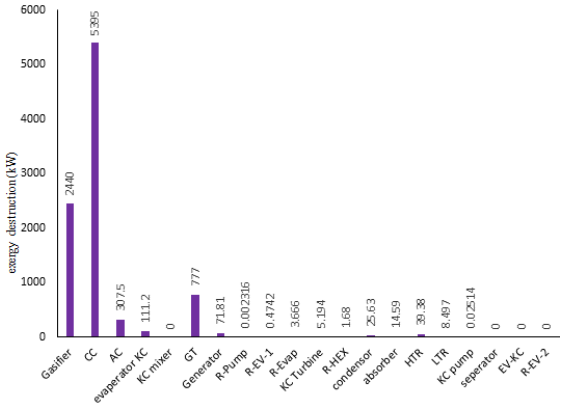

Figure 11. Exergy destruction rates of hybrid system components

F. Environmental Impact

To evaluate the environmental impact, carbon dioxide production was compared in power generation, combined power and heat generation and tri-generation in a proposed hybrid system. Figure 11 compares the desirable output and carbon dioxide emission of the hybrid system.

According to Figure 11, it is clear that the hybrid system produces less carbon dioxide and yields more. Accordingly, this system generates 0.75 and 1.4 (tons per MWh) less carbon dioxide generation compared to the single power system. These values indicate the advantage of the hybrid system.

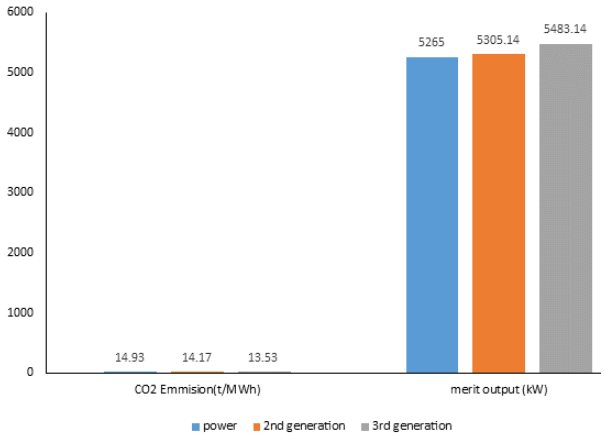

Figure 12. Comparison of desirable output and carbon dioxide emission of hybrid system

APPENDICES

Table 1. Mass and energy balances terms of first part of the hybrid system

Exergy Balance	Energy Balance	Component
Air Compressor	$\dot{m}_1=\dot{m}_2$	$\eta_{is,AC}=\frac{W_{is,Ac}}{W_{AC}},\ W_{AC}=\bar{h}_2-\bar{h}_1$
Gas Turbine	$\dot{m}_3=\dot{m}_4$	$\eta_{is,GT}=\frac{W_{is,GT}}{W_{GT}},W_{GT}=\bar{h}_3-\bar{h}_4$

Table 2. Exergy destruction terms for system components

Component	Exergy Destruction
Gasifier	$\dot{E}_{D,G}=\dot{E}_5+\dot{E}_6-\dot{E}_7$
Combustion Chamber	$\dot{E}_{D,G}=\dot{E}_5+\dot{E}_6-\dot{E}_7$
Gas Turbine	$\dot{E}_{D,GT}=\dot{E}_3+\dot{E}_4-\dot{E}_{GT}$
Compressor Air	$\dot{E}_{D,AC}=\dot{E}_1+\dot{E}_2-\dot{E}_{AC}$

Table 3. Final analysis and calorific value of the biomass used in this study

Higher Heating Value (KJ/Kmol)	Ash	O	S	N	H	C	Biomass
449,568	-	44	0	0	6	50	Wood

Table 4. Mass balance equations of energy for Kalina cycle

Component	Exergy destruction
Turbine	$\eta_{is,T}=\frac{W_{is}}{W_a}\ ,\ \dot{W}_T=\dot{m}_{24}(h_{24}-h_{25})$
Evaporator	$\dot{m}_{16}\left(h_{16}-h_{17}\right)=\dot{m}_{22}\left(h_{23}-h_{22}\right)$
Separator	$\dot{m}_{23}h_{23}=\dot{m}_{24}h_{24}+\dot{m}_{26}h_{26}$
Condenser	$\dot{E}_{D,AC}=\dot{E}_1+\dot{E}_2-\dot{E}_{AC}$
Pump	$\eta_{is,P}=\frac{W_a}{W_{is}}\ ,\ \dot{W}_P=\dot{m}_{22}(h_{20}-h_{19})$
HTR	$\dot{m}_{22}\left(h_{22}-h_{21}\right)=\dot{m}_{26}\left(h_{27}-h_{26}\right)$
LTR	$\left(h_{29}-h_{30}\right)=\left(h_{21}-h_{20}\right)$

Table 5. Exergy balance equations for Kalina cycle

Component	Exergy Destruction Rate Expression
Turbine	$\dot{E}_{D,T}=\dot{E}_{23}-\dot{E}_{24}-\dot{W}_T$
Evaporator	$\dot{E}_{D,Ev}=\dot{E}_{21}-\dot{E}_{22}+\dot{E}_4-\dot{E}_{exit,evap}$
Separator	$\dot{E}_{D,Sep}=\dot{E}_{22}-\dot{E}_{23}-\dot{E}_{25}$
Condenser	$\dot{E}_{D,Con}=\dot{E}_{29}-\dot{E}_{18}$
Pump	$\dot{E}_{D,P}=\dot{E}_{18}-\dot{E}_{19}+\dot{W}_p$
HTR	$\dot{E}_{D,HTR}=\dot{E}_{25}+\dot{E}_{20}-\dot{E}_{26}-\dot{E}_{21}$
LTR	$\dot{E}_{D,LTR}=\dot{E}_{28}+\dot{E}_{19}-\dot{E}_{20}-\dot{E}_{29}$

Table 6 Energy balance equations for components of Lithium-bromide absorption refrigeration cycle

Component	Energy Balance
G	$\dot{Q}_G=\dot{m}_{34}h_{34}+\dot{m}_{37}h_{37}-\dot{m}_{33}h_{33}$
Evap	$\dot{Q}_{evap}=\dot{m}_{40}h_{40}-\dot{m}_{39}h_{39}$
Cond	$\dot{Q}_{cond}=\dot{m}_{37}h_{37}-\dot{m}_{38}h_{38}$
Abs	$\dot{Q}_{abs}=\dot{m}_{36}h_{36}+\dot{m}_{40}h_{40}-\dot{m}_{31}h_{31}$
Pump	$h_{32}=h_{31}+\frac{\dot{W}_p}{\dot{m}_{31}}\ ,\ \dot{W}_p=\dot{m}_{31}\times\left(P_{HPG}-P_{abs}\right)/\eta_p\times\rho_{31}$
HEX	$h_{34}=h_{35}-\left(h_{35}-h_{34}^{'}\right)\times\eta_{HEX}\ ,\ h_{36}=\frac{\dot{m}_{35}}{\dot{m}_{36}}\left(h_{35}-h_{34}\right)+h_{32})$
EV	$h_i=h_e$

Table 7. Energy balance equations for components of Lithium-bromide absorption refrigeration cycle

Component	Exergy Destruction Rate Expression
G	$\dot{E}_{D,G}=\dot{E}_{33}-\dot{E}_{37}-\dot{E}_{34}+\dot{E}_{in\ gas}-\dot{E}_{out\ gas.}$
Evap	$\dot{E}_{D,evap}=\dot{E}_{39}+\dot{E}_{52}-\dot{E}_{53}-\dot{E}_{40}$
Cond	$\dot{E}_{D,Cond}=\dot{E}_{37}+\dot{E}_{50}-\dot{E}_{38}-\dot{E}_{51}$
Abs	$\dot{E}_{D,Abs}=\dot{E}_{40}+\dot{E}_{36}+\dot{E}_{54}-\dot{E}_{31}-\dot{E}_{55}$
Pump	$\dot{E}_{D,P}=\dot{E}_{31}-\dot{E}_{32}+\dot{W}_p$
HEX	$\dot{E}_{D,HEX}=\dot{E}_{34}+\dot{E}_{32}-\dot{E}_{35}-\dot{E}_{33}$
EV	$\dot{E}_{D,EV}=\dot{E}_i-\dot{E}_e$

Table 8. The obtained results of the present study compared with the empirical results

Constituent	Present Model	Experiment [1]	Zainal Equilibrium Model [5]
Hydrogen	21.60	15.23	21.06
Carbon Monoxide	20.48	23.04	19.61
Methane	1.03	1.58	0.64
Carbon Dioxide	12.40	16.42	12.01
Nitrogen	44.48	42.31	46.68
Oxygen	0	1.42	0

Table 9. Comparison of the results of the present work with others

Present work	Refs. [16, 17]	
KC parameters		
2186.1	2194.6	Net power output (kW)

IV. CONCLUSIONS

This study aimed to propose a combined tri-generation system with the least environmental impact and the highest efficiency to produce power through renewable energy and to compare it with the configurations presented in the literature.

This contains a parametric study of effective quantities on the cycle and the obtained results are as follows:

1. System efficiency for tri-generation system was greater, but environmental impact was less that should be considered in the design.
2. System performance is optimized for upper and lower power generation system at certain pressure ratios.
3. With increasing the gas turbine inlet temperature (which is useful for system performance), the optimum pressure tends to lower values.
4. The use of absorption refrigeration cycle has a significant impact on the first law performance of the system.
5. The second law efficiency is the best target function to optimize the system due to taking energy quality into account.
6. 5265 kW power, 178 kW cooling and 41 kW heat was generated in the introduced system.

ACKNOWLEDGEMENTS

Many thanks to the great supporting of Acad. Arif M. Hashimov and Prof. Fegan Q. Aliyev as the doctoral thesis supervisors and other parts for power research opportunities at University of Baku, Baku, Azerbaijan, was a great help for developing this paper. With the cooperation of the Ph.D. thesis's supervisor Acad. Arif M. Hashimov that spent a valuable part of his time for the paper.

REFERENCES

[1] M.J. Moran, H.N. Shapiro, D.D. Boettner, M.B. Bailey, "Fundamentals of Engineering Thermodynamics", John Wiley & Sons, 2010.

[2] A. Bejan, G. Tsatsaronis, "Thermal Design and Optimization", John Wiley & Sons, 1996.

[3] J. Szargut, T. Styrylska, "Approximate Evaluation of the Exergy of Fuels", Brennst. Warme Kraft, Vol. 16, No. 12, pp. 589-596 1964.

[4] T.J. Kotas, "The Exergy Method of Thermal Plant Analysis", Elsevier, 2013.

[5] Z.A. Zainal, R. Ali, C.H. Lean, K.N. Seetharamu, "Prediction of Performance of a Downdraft Gasifier Using Equilibrium Modeling for Different Biomass Materials", Energy Conversion and Management, Vol. 42, No. 12, pp. 1499-1515, 2001.

[6] R.H. Perry, D.W. Green, J.O. Maloney, M.M. Abbott, C.M. Ambler, R.C. Amero, et al., "Perry's Chemical Engineers", Handbook, Vol. 7, McGraw-Hill, New York, 1997.

[7] P. Basu, "Biomass Gasification and Pyrolysis: Practical Design and Theory", Academic Press, 2010.

[8] S. Soltani, S.M.S. Mahmoudi, M. Yari, M. Rosen, "Thermodynamic Analyses of a Biomass Integrated Fired Combined Cycle", Appl. Therm. Eng., Vol. 59, pp. 60-68, 2013, doi:10.1016/j.applthermaleng.2013.05.018.

[9] K.J. Ptasinski, M.J. Prins, A. Pierik, "Exergetic Evaluation of Biomass Gasification", Energy, Vol. 32, pp. 568-574, 2007, doi:10.1016/j.energy.2006.06.024.

[10] M.J. Prins, K.J. Ptasinski, F.J.J.G. Janssen, "From Coal to Biomass Gasification: Comparison of Thermodynamic Efficiency", Energy, Vol. 32, pp. 1248-1259, 2007.

[11] P. Ahmadi, I. Dincer, M. Rosen, "Development and Assessment of an Integrated Biomass-Based Multi-Generation Energy System", Energy, Vol. 56, pp. 155-166, 2013, doi:10.1016/j.energy.2013.04.024.

[12] A. Datta, R. Ganguly, L. Sarkar, "Energy and Exergy Analyses of an Externally Fired Gas Turbine (EFGT) Cycle Integrated with Biomass Gasifier for Distributed Power Generation", Energy, Vol. 35, pp. 341-350, 2009-2010.

[13] E. Gholamian, V. Zare, "A Comparative Thermodynamic Investigation with Environmental Analysis of SOFC Waste Heat to Power Conversion Employing Kalina and Organic Rankine Cycles", 2016.

[14] P. Tatsidjodoung, M.H. Dabat, J. Blin, "Insights into Biofuel Development in Burkina Faso: Potential and Strategies for Sustainable Energy Policies", Renew Sustain. Energy Rev., 2012.

[15] Z.A.Z. Alauddin, "Performance and Characteristics of a Biomass Gasifier System", Ph.D. Diss., University of Wales, Cardiff, 1996.

[16] S. Ogriseck, "Integration of Kalina Cycle in a Combined Heat and Power Plant," A Case Study", Applied Thermal Engineering, Vol. 29, No. 14, pp. 2843-2848, 2009.

[17] M. Yari, "Exergetic Analysis of Various Types of Geothermal Power Plants", Renew. Energy, 2010.

[18] R. Gomri, R. Hakimi, "Second Law Analysis of Double Effect Vapour Absorption Cooler System", Energy Convers. Manag., Vol. 49, pp. 3343-3348, 2008.

[19] S. Soltani, S.M.S. Mahmoudi, M. Yari, M. Rosen, "Thermodynamic Analyses of an Externally Fired Gas Turbine Combined Cycle Integrated with a Biomass Gasification Plant", Energy Convers. Manag., Vol. 70, pp. 107-115, 2013, doi:10.1016/j.enconman.2013.03.002.

BIOGRAPHY

Alireza Salimi was born in Urmia, Iran, 1966. He received the B.Sc. and the M.Sc. degrees in the field of Physics from International City University in 2011, 2014, respectively. Currently, he is the Ph.D. student of Physics in Institute of Physics, Azerbaijan National Academy of Sciences, Baku, Azerbaijan. He is a Lecturer Assistant of Physics at Urmia Branch, Islamic Azad University, Urmia, Iran and teaches physical science. His research interests are in the area of physics, mechanics, and thermodynamics.